RESEARCH ARTICLE | OCTOBER 04 2022

Simulation of grid morphology's effect on ion optics and the local electric field

Z. Levin ; S. Kempf

AIP Advances 12, 105002 (2022)
https://doi.org/10.1063/5.0084142
CHORUS

Simulation of grid morphology's effect on ion optics and the local electric field

Cite as: AIP Advances 12, 105002 (2022); doi: 10.1063/5.0084142
Submitted: 5 May 2022 • Accepted: 4 August 2022 •
Published Online: 4 October 2022

Z. Levin[a] and S. Kempf[b]

AFFILIATIONS

Laboratory for Atmospheric and Space Physics, University of Colorado, Boulder, Colorado 80303, USA and Solar System Exploration Research Virtual Institute (SSERVI) - Institute for Modeling Plasmas, Atmospheres, and Cosmic Dust (IMPACT), University of Colorado, Boulder, Colorado 80303, USA

[a]Author to whom correspondence should be addressed: Zuni.Levin@LASP.colorado.edu
[b]Sascha.Kempf@lasp.colorado.edu

ABSTRACT

Electric field ion optics are employed by many scientific instruments for investigating ions, e.g., using time-of-flight mass spectrometers. A common design feature of such instruments is the grounded grid that provides boundaries between regions that need to have different electric fields. In order to save computer memory, these grids are often modeled by indefinitely thin conducting sheets. This approximation does not include the effects of the grid morphology on the electric field. This paper investigates these grid morphology effects on both the electric field and the trajectories of ions passing through the grids using finite element analysis. The simulations in this paper indicate that a significant amount of the electric potential will leak through a grid's empty space. The leakage of this field through the grid slows an ion down relative to the speed that it would be assumed to have based on the indefinitely thin sheet model. The ions are then eventually accelerated back to the energy that they would have if the grid were a thin sheet. However, this deceleration and acceleration result in the lengthening of the ion time of flight, independent of the size of the drift region. The deflection of the ions passing through the grid increases with the ion's proximity to the grid struts, the size of the acceleration region, and the shape of the grid cell. This deflection also results in a small but potentially significant loss of focus and changes in the path length.

I. INTRODUCTION

SIMION is a piece of software that is often used for the simulation of ion optics. SIMION recommends that, so as to save computer memory, grids should be modeled as if they were indefinitely thin sheets that are transparent to the motion of ions but have opaque to electric fields. This suggested approximation method is intended to save a considerable amount of computer RAM that it takes to model realistic grids.[1] A thorough examination of the literature on the topic of grids—the effects of grids on ion optics—also shows the prevalence of a method of modeling a realistic 2-dimensional cross section of a grid as an approximation of a 3-dimensional grid.[2–4] SIMION was used in the study by King and by Selby *et al.*[2,3] while the study by Lewin *et al.* used I-OPT to simulate the parallel wire grid's effect on the trajectories of ions passing through a grid and used SIMTOF to determine its simulated spectra.[4] This method of approximation does a better job of resolving the grid morphology than SIMION's suggestion of an indefinitely thin sheet but it still does not capture the entirety of a realistic grid design's effect on ion optics because it equates different grid cell shapes that have the same cross-sectional area as each other. A square grid cell with 1 mm sides will be the same as a circle grid cell with 1 mm diameter under such a 2-dimensional cross section, as will a hexagon with an edge-to-edge distance of 1 mm.

The purpose of the computer simulations performed for this paper is to explore how a grid cell's 3-dimensional morphology changes the local electric field and how these changes affect the velocities and trajectories of ions passing through the grid. In particular, one of the principle objectives of this paper is to determine how accurate the approximation of a grid as an indefinitely thin sheet is for a variety of 3-dimensional grid cell designs. This paper will also evaluate the accuracy of the approximation of a grid as a 2-dimensional model by demonstrating that there are differences between grid cells that have the exact same 2-dimensional cross sections. The 3-dimensional grid cells that will be explored in this paper

are a selection of square grid cells that have the same side-length, similar to the diameter of a selection of circle grid cells and hex grid cells that have the same edge-to-edge distance as the side length of the square grid cells.

II. METHODS: ELECTRIC FIELD PERTURBATIONS DUE TO THE GRID STRUCTURE

Figure 1 shows the generic instrument that is modeled for the purpose of exploring the effects of the grid morphology. This model is kept constant except for the grid that is modeled as either an indefinitely thin grounded plane or a grounded parallel grid with different shapes and sizes of grid cells. This grid is situated at a distance of L = 24.8 mm from the target electrode that is charged to a potential bias of 3000 V. SIMION simulations are then performed, which show that calculating the electric field formed between the potentially biased electrode and the grid is effective for determination of the ion optics characteristics of instruments.[5] SIMION is a piece of commercial software used for performing ion optics simulations via the numerical calculation of static and quasistatic electric fields.

SIMION finds the electric field by solving the Poisson equation $\nabla \cdot (\varepsilon_r E) = -\frac{\rho}{\varepsilon_0}$ employing finite difference methods. In this paper, all simulations are performed using no space charge and no dielectric components, so the Poisson equation reduces to the Laplace equation $\nabla \cdot E = 0$. SIMION defines its electrodes, both biased and grounded, as a series of voxels, which may be cubes or rectangular cuboids and may or may not be transparent to ions but are always treated as a Dirichlet boundary condition (i.e., the potential is held constant across the surface of the electrode).[1] By default, SIMION employs von Neumann boundary conditions (zero electric field) for the edges of the simulation domain. In this paper, Dirichlet boundary conditions are applied by replacing the domain boundaries with grounded electrodes to ensure uniqueness of the field solution.[6]

First, consider the case of the unperturbed field, i.e., the field formed between two parallel solid electrodes where one is given a potential bias and the other is grounded. Circular electrodes with a radius of 50 mm are placed within a grounded cylinder to minimize any fringing effects from the simulated chamber's walls. The grounded electrode is made into an indefinitely thin sheet and is made transparent to simulated ions while still being opaque to electric fields. This change allows us to simulate not just the "acceleration region" between the biased electrode and the grounded electrode

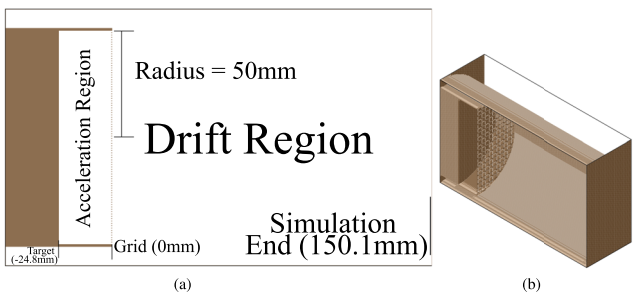

FIG. 1. (a, left) Simulated model's cross section except for the expanded and shortened acceleration regions seen in Fig. 7 and (b, right) 3-dimensional cutaway from an isometric perspective.

but also to see the effects on the ion's trajectory after it leaves the acceleration region. The field generated in this setup is effectively uniform near the center of the simulated instrument, and an ion traveling from the biased targeted plate to the grounded plate will acquire 100% of the potential energy in the electric field as kinetic energy by the time that it arrives on the grounded electrode.

Now the grounded indefinitely thin solid electrode is replaced by a realistic model of a grid. As a consequence, the electric potential will no longer be zero anywhere within the grid plane (Fig. 2), and the electric field is no longer simply orthogonal to the grid plane. Ions moving in this field are affected in three ways: their time-of-flight from the solid electrode to the grid plane is now dependent on the potential field leaking through the grid plane, which will be referred to as "potential leakage," the ions do not gain 100% of the kinetic energy that they will gain from the field by the time the ion passes through the grid plane, and the ions' velocity vectors are deflected off of their initial trajectories by their attraction toward the grid struts. These three effects are all of concern for the performance of ion optics, in particular for the design of the acceleration region in time-of-flight mass spectrometers, which are intended to generate a thin ion beam orthogonal to the grid plane with a minimal time-of-flight spread.[7]

Grids were simulated with varying grid cell size and grid cell morphology (square, circular or hexagonal shape). The electric field is produced by a 3000 V biased electrode located 24.8 mm from the nearest edge of the grid. This simulation was also performed with five ring electrodes designed to smoothen the electric field inside the acceleration region, which had no non-negligible effect on the potential leakage, which follows because the electric field contributions from the ring electrodes are almost entirely parallel to the grid plane and therefore does not contribute much to the field inside the grid cells. Altering the thickness of the grid struts made a small change that is visible, as shown in Fig. 2. These models only represent the effect of the electric field emanating from within the acceleration region and do not take into account any electrodes that might be in the drift region of a real scientific instrument.

It should be noted that the potential leakage cannot be accurately modeled as a plate with just a single grid cell of open space since this will force the electric field through a tighter space, which will increase it as compared to modeling the full grid. The exact extent of the changes in the electric field that comes from using this method is beyond the scope of this paper; however, cursory examination shows that this method fails to reproduce the equipotential lines seen in Fig. 2, and as such, the full simulation of the grid morphology shown in Fig. 1 is used.

All ions were launched under the initial conditions of 100 amu mass, 1 eV kinetic energy, and +1 eV charge with the velocity aligned parallel to the boresight.

III. DISCUSSION: GRIDS IN GENERALIZED MASS SPECTROMETER SIMULATION RESULTS

A. Effects of potential leakage on the time of flight of ions

Figure 3 (see Fig. 8 in the Appendix for a zoomed-in view) shows that the ion gains from the acceleration region (i.e., a gained

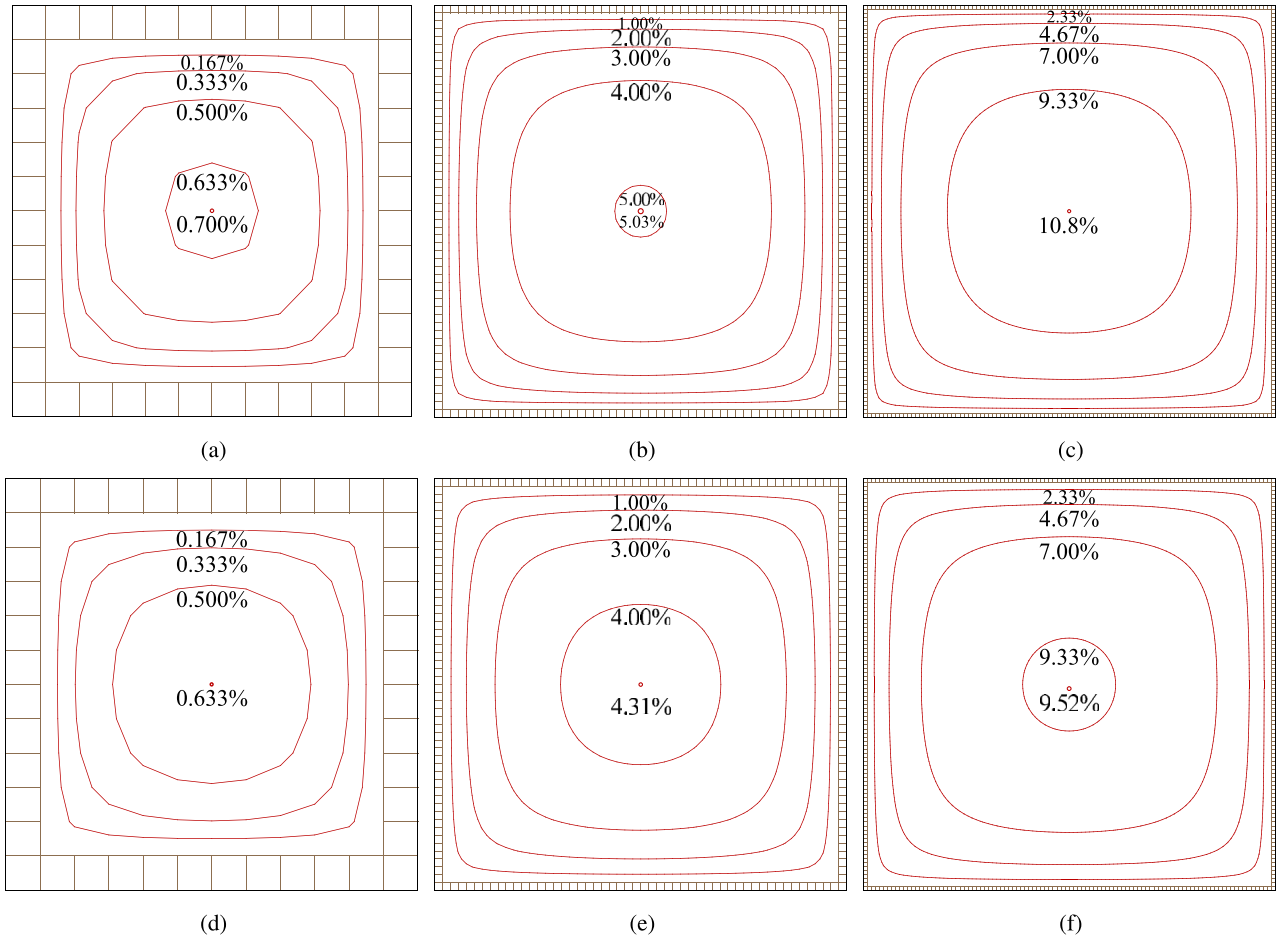

FIG. 2. Equipotential lines for square grid cells that each have struts 0.1 mm thick and have sides of inner lengths of (a, top-left) 1 mm, (b, top-middle) 5 mm, and (c, top-right) 10 mm as well as square grids that have each have struts 0.5 mm thick and have sides of inner lengths of (d, bottom-left) 1 mm, (e, bottom-middle) 5 mm, and (f, bottom-right) 10 mm, which demonstrates the effect of the grid morphology that is dependent on the thickness of the grid struts. Below each equipotential line, the percentage of the target's potential bias that is slipping through the grid cell is written. Note that the rest of the graphs in this paper will use 0.1 mm grid struts.

velocity pointing along the boresight of the acceleration region). The ion gains relatively more kinetic energy the closer it gets to the grounded structure of the grid. The larger the grid cell size, the larger the electric flux passing through the grid cell. The ion does not gain all the potential energy granted to it by the potential difference between the target and the ground in the acceleration region of a mass spectrometer until after it passes through the grid since the acceleration region's electric field extends beyond the grid's opening.

Figure 4 (see Fig. 10 in the Appendix for a zoomed-in view) shows that the effect of this delay in regaining the ion's kinetic energy is that the ion is traveling slower relative to how fast the ion would be traveling by the time it passes through the grid. Simulations showed that the kinetic energy of an ion at the center of a grid is proportional to the square of the distance between itself and the grid struts.

Increasing the amount of open space in a grid proportionally increases the probability that an ion will successfully move through the grid. However, an increase in the open space of a grid can also reduce the ratio of the ion's energy with the grid morphology taken into account to the ion's energy with the grid approximated by an indefinitely thin sheet by 10.8 percentage points for square grid cells with 10 mm on each side separated by 0.1 mm thick struts, which are 0.2 mm deep. The circle grids performed better than the square grids, where they reduce the time-of-flight, and the kinetic energy acquired by the ion is less than that acquired by the square grids while also having minimum deflection. However, circle grids also have a smaller open area that is $\frac{\pi}{4}$ times the size of the open area of a square grid with the side length equal to the circle grid's diameter. The ion is deflected toward the grid in a direction orthogonal to the instrument's boresight because of the change in the shape of

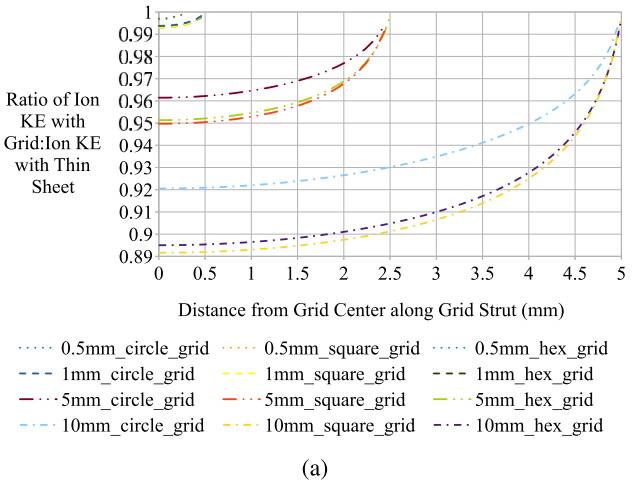

(a)

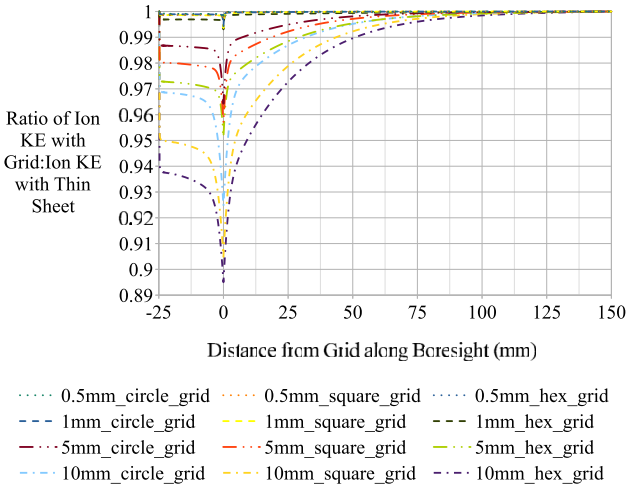

(b)

FIG. 3. (a, top) Ion kinetic energy decreases when the ion passes closer to the struts of the grid structure and asymptotically approaches 100% of the kinetic energy that it would have if a thin sheet is used for the grid. The ion launched in this simulation that is closest to the grid struts is always launched at a position that is 0.1 mm from the grid struts (except for the 10 mm circle grid for which the ion hits the grid structure if the ion is launched 0.1 mm from the grid strut so the launch location of 0.2 mm away from the grid strut is the final point in this graph). (b, bottom) The simulations also shows that the ion's kinetic energy is minimized when it is in the plane of the grid, and it regains the kinetic energy that it lost in the grid very quickly for 1 mm grid cells, but for 10 mm grid cells, it takes about $\frac{2}{3}$ of the size of the region beyond the accelerating grid for it to recover all the kinetic energy that it would have gotten immediately upon exiting the sheath grid.

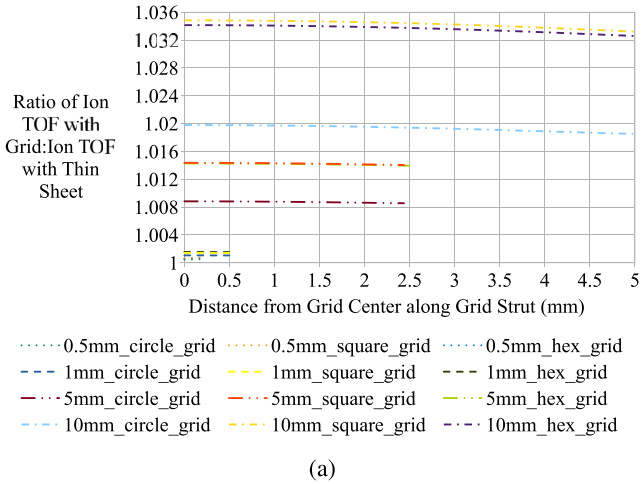

(a)

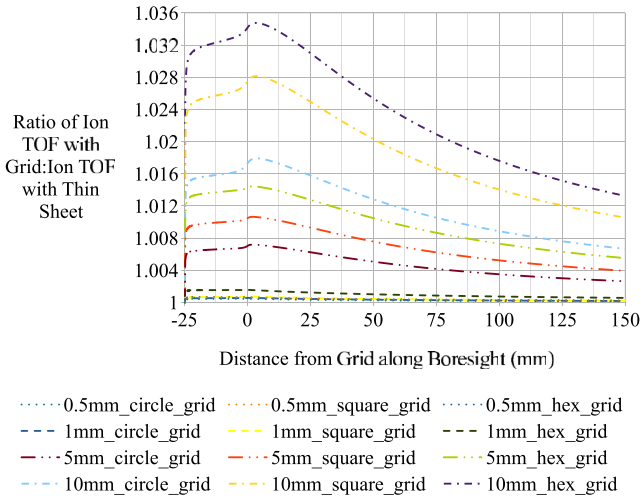

(b)

FIG. 4. (a, top) Ion's Time-of-Flight (TOF) with the grid morphology modeled is always higher than the ion's TOF when the grid morphology is approximated as a thin sheet, and the TOF is almost constant across the grid cell. (b, bottom) When simulated as traveling along the boresight, the ion with the grid morphology modeled starts out slower than the one without the grid, but then the ion starts to accelerate a short distance after it clears the grid; importantly, however, the ion does not necessarily recover its full TOF by the time it gets to the 0 V potential point at the end of the simulated instrument.

the electric field due to the grounded grid being at a lower potential bias relative to the potential at the center of each grid cell. Figure 6 shows a difference in the deflection that seems to be due to the shape of the grid cells.

B. Path deflection of ions by potential leakage

Figure 5 (see Figs. 9 and 11 in the Appendix for a zoomed-in view) shows that the deflection increases at a constant rate of $0.6 \pm 0.11 \frac{degree}{mm}$, with square grids always causing more deflection than both circle grids and hex grids of the same 2-dimensional cross-sectional profile. There is effectively a linear relationship for the deflection as it increases from the 0 deflection seen with ions at the center of the grid cell to the ion's maximum deflection when it is very close to the grid cell strut. The path deflection of the ions happens rapidly after they pass close to the grid struts. The deflection of the ions increases as the ion approaches the grid struts. At most, the deflection caused by a 10mm-sided grid cell will trace out an arc segment of $0.03r$, where r is the radius of the arc segment.

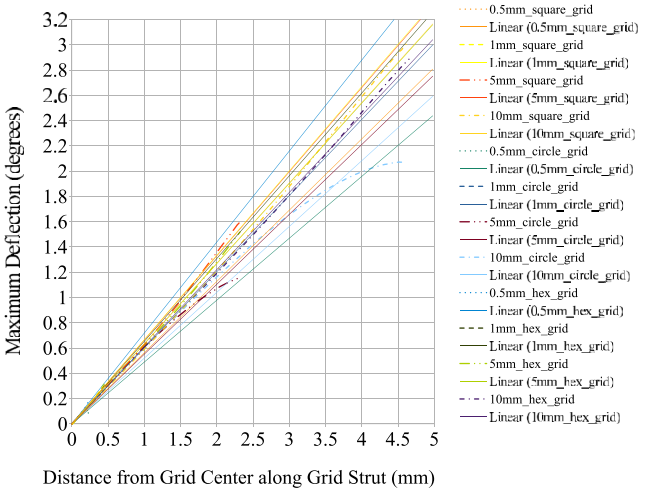

(a)

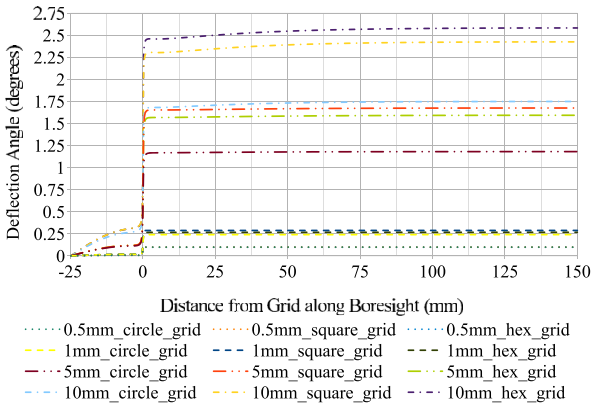

(b)

FIG. 5. (a, top) There is a roughly linear trend to the amount of deflection of an ion depending on its distance from its grid center as measured along the grid struts. Linear regressions were performed on each of the lines, and the results of such are shown next to the figures in the legend, where x is the distance from the grid along the grid struts (note that in the models that are being used in this paper, this distance would be along the y-axis, and the boresight is along the x-axis) and $f(x)$ is the maximum deflection when it is approximated as a linear function of x. From the top to the bottom of the plots shown in the legend, $f(x) = 0.5639x, 0.6667x, 0.6653x, 0.6357x, 0.4897x, 0.6024x, 0.5527x, 0.5207x, 0.7199x, 0.6546x, 0.6345x$, and $0.6107x$ These approximations are close enough such that one may use the equation to figure out the deflection. (b, bottom) The deflection of the ions' velocities increases quickly and then levels off as they travel along the boresight, so the maximum deflection will only be modeled based on the maximum deflection that, in these simulations, is attained at 5 mm from the grid in the direction that is along the boresight.

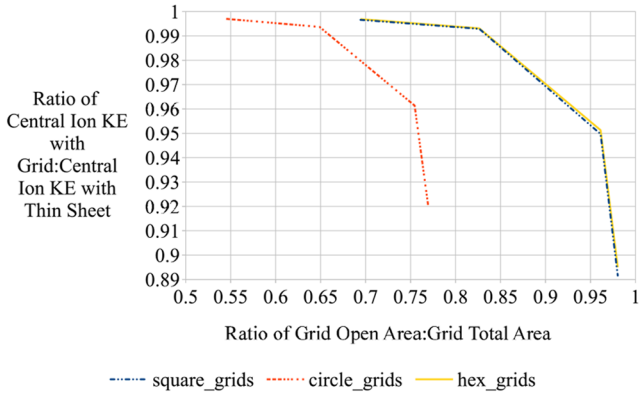

(a)

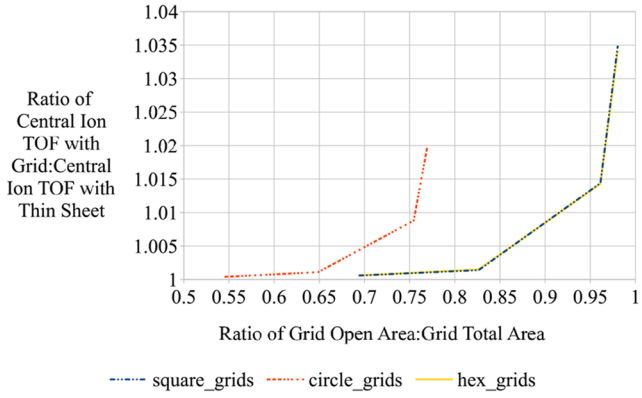

(b)

FIG. 6. (a, top) As the grid open area increases, the potential leakage (shown here as the change in an ion's kinetic energy relative to the ion's kinetic energy when the grid morphology is approximated as a thin sheet) increases, but there is also some dependency on the shape of the grid cell. Note that the sharp elbows on this graph each represent one of the four data points used to make this graph. (b, right) This graph is of the ion's relative change in time-of-flight instead of kinetic energy. It is not surprising that the time-of-flight graph has the same shape as the kinetic energy graph, mirrored and stretched, because the changes in kinetic energy here come entirely from the changes in velocity. Note that both the graphs use an ion flying through the exact center of the grid cell where the potential leakage is highest.

C. Effects of grid open area and grid cell shape on potential leakage

In Fig. 6, the plot representing the square grid cells and the plot representing the hex grid cells almost perfectly overlap. All three grid shapes have the same 2-dimensional cross-sectional profile, but they behave differently once their 3-dimensional shapes are taken into account. The dominant factor responsible for the kinetic energy and time-of-flight differences is the open area of the grid; however, the shape of the grid cell is also relevant. The circle grids have significantly higher potential leakage than the hex or square grids even in the case where the circle grids have more open area than the hex grid. The key determinant of the potential leakage is neither the shape nor the grid cell's open area, but rather it is the packing efficiency of the grid cells that is most significant. The packing efficiency is a simple function of the grids' geometry and for both square grids and hex grids that are packed together in the most efficient manner possible, with the 0.1 mm grid struts being used. The grid's empty area

is $\frac{L^2}{P^2}$, where L is the length of a square grid cell's side or the distance from edge-to-edge of a hexagon since these produce the same 2-dimensional profile and P is the pitch (i.e., the distance from one grid cell's center to the adjacent grid cell's center with the thickness of the grid struts included). The circle cell grid that was used in this paper has the same pitch as the square grid and the same pattern of hole placement (i.e., along the lines parallel to either the y or z axis in a square formation when the boresight is along the x-axis), but the circle grid's open area is $\frac{\pi}{4}\frac{r^2}{P^2}$, where r is the circle grid cell's radius.

IV. REDUCTION OF THE RELATIVE LOSS OF KINETIC ENERGY AND TIME-OF-FLIGHT VIA LENGTHENED ACCELERATION REGIONS

Figure 1(a) is an illustration of the acceleration region, which is defined as a general part of an instrument with a biased target plate where an ion is generated, such as in impact ionization mass spectrometers,[8] that is bounded by a grounded grid. Figure 7 shows that the kinetic energy lost to the grid was substantially reduced by lengthening the distance from the target to the grid to 50.8 mm, which caused the 10 mm square grid cells' effect on kinetic energy to decrease to 3% less than that of a thin sheet grid and a TOF of 0.4% more than that of the thin sheet grid. While the potential difference between the target and the grid is the same with every length of the acceleration region, the electric field is stronger since the electric field is proportional to $\frac{1}{r^2}$ while the potential is proportional to $\frac{1}{r}$. The grid struts can only absorb a finite amount of electric flux, so a strong electric field will be reduced by the grid less than a weak electric field will do.

V. AN ANALYTICAL SHORTCUT FOR THE DESIGN OF ACCELERATION REGIONS

Simulations highlighted in Fig. 2 show that while the value of the potential at the center of the grid cell is variable, the ratio of the potential at the center of the grid cell to the potential bias on the target electrode is constant with respect to changes to the target electrode's potential bias. Accurate simulation of the grid morphology requires numerical methods because an entire grid is often too asymmetrical to be solved with analytical methods. However, many grid regions can be derived from a single numerical simulation via the following equation:

$$\frac{V_{PL_A}}{V_{T_A}} = \frac{V_{PL_B}}{V_{T_B}}. \tag{1}$$

Here, V_{PL} is the potential at the center of the grid cell (i.e., the potential leakage at the grid cell's center), and V_T is the potential bias that the target is set to. A numerical simulation must be used to calculate V_{PL_A}, but afterward, one is free to use this equation to quickly optimize an instrument's acceleration region according to one's specifications. This equation only applies when the grid cell and the geometry of the acceleration region are constant. In order to change $\frac{V_{PL}}{V_T}$, it is necessary to change the geometry of the grid cell and/or the acceleration region. Note that simulations of changes to the geometry of the drift region were not shown to affect $\frac{V_{PL}}{V_T}$. Since the electric potential is proportional to the charge as per Coulomb's law, $V = \frac{1}{4\pi\varepsilon_0}\frac{q}{r}$, it is necessary that an increase in the charge (q) would increase the electric potential as well, and since the target is the only source of potential, the fraction $\frac{V_{PL}}{V_T}$ must remain the same.

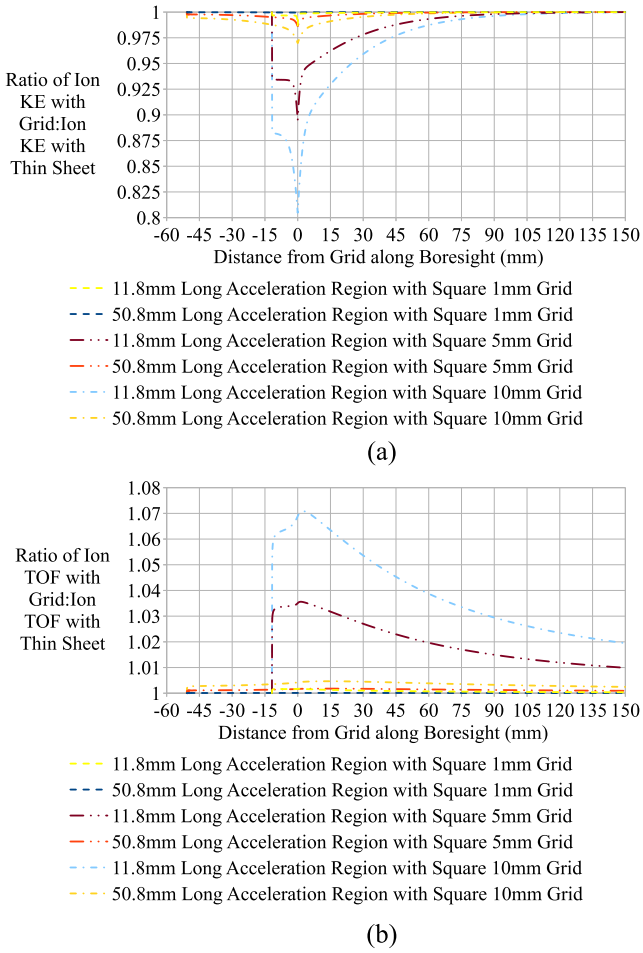

FIG. 7. (a, top) Effect of the lengthening and shortening of the acceleration region measured along the boresight with the ratio of the ion's kinetic energy with the grid modeled with cells to thin sheet grid-approximations. (b, bottom) The ratio of the ion's time-of-flight with the grid and without the grid is also shown for square grids. While the ions always recover their kinetic energy, the time-of-flight is not fully recovered at the end of the instrument due to the extra time that the ion spends accelerating and decelerating at slower rates than in the case where the grid is a thin sheet.

VI. AVAILABILITY

To replicate these simulations, all that is required is a piece of numerical simulation software capable of solving the Laplace equation $\nabla \cdot E = 0$ in a sufficiently detailed 3D space. This can require a moderate-to-large amount of RAM depending on the

details required. The square grid and circle grid simulations in this paper were run comfortably on a computer with 16 GB of RAM installed, of which 6.89 GB was required for the models used. The more details that are modeled in the simulation will improve the accuracy of results but might require higher amounts of RAM. Structures in SIMION are the easiest to accurately simulate if they are definable by a set of equations with only one non-piecewise equation for each of the x, y, and z coordinates, such as in the circle, or if the structures run parallel to the coordinate axes, which allows for easy simulation of square grids in SIMION. Hexagons have straight diagonal lines (i.e., lines that are neither parallel nor orthogonal to at least two coordinate axes), which are in neither of the prior two categories, so they are difficult for SIMION to simulate and require more RAM; otherwise, the diagonal lines will have to be approximated by a jagged staircase-like line. The hex grid simulations were carried out on a computer with 58 GB of RAM installed, of which 55.58 GB was required for the hex model that should well-approximate such diagonal lines.

VII. CONCLUSIONS

In summary, this paper provides several simulations that investigate the effects of grid morphology on the time-of-flight, ratio of kinetic energy to potential energy, and trajectory of ions passing through a grid. The grids with more free space will let through more of the electric field as potential leakage. However, square and hex grids deflect ions more than circular grids do when the ions are closer to the edge of the grid cell since the square edge always has the same edge area for exerting a deflecting force on the ion. In the case of circle or hex shaped grid cells, the closer that an ion gets to the edge of a circle or a hex grid cell, the more components of the electric field pointing orthogonal to the ion's trajectory are passed-by, and a smaller area will be exerting a smaller Coulomb force on the ion than in the square grid cell case. This can be seen in Fig. 5(b) (see Fig. 11 in the Appendix for a zoomed-in view), in which the circle grids have less linearity and are falling off as the ion approaches the grid strut. Remedying this effect is easy if one procures a grid with 1×1 mm^2 squares, or if collection efficiency is more important for the particular instrument, this effect can be remedied by using a sparse grid with an increased acceleration region length.

The ion's energy is, of course, always conserved, and the ion regains its initial kinetic energy by the end of the instrument. However, potential leakage means that the ion will not regain the entirety of the kinetic energy that it gets from the acceleration region by the time it reaches the grid. The ion's kinetic energy converges to 100% of the potential bias of the target that the ion starts due to conservation of energy.

It is key that while the ion's time-of-flight does converge in several solutions, the time-of-flight does not converge where it would be under the approximation of a grid as an indefinitely thin sheet. An ion's time-of-flight is not strongly affected by how close the ion is to the grid struts; instead, the ion's time-of-flight is only affected by the size and shape of the grid cell. It should be noted that grid effects on the time-of-flight are additive, so an instrument with many grids might experience significant TOF delays.

Investigations into remedying these effects for instruments of various needs have shown that lengthening the acceleration region significantly improves the results and is a good option for instruments that want to maximize the open area in their grids. Instruments that have to make use of short acceleration regions are also viable, but they must compensate via a reduced grid size relative to instruments with long acceleration regions.

An application of these findings is found in time-of-flight mass spectrometry, which is dependent on the predictability of the time-of-flight of ions,[7] which can be disrupted by the need to recover kinetic energy over a significant drift length relative to the sides of each grid cell (see Fig. 3) (see Fig. 8 in the Appendix for a zoomed-in view). In an impact-ionization mass spectrometer, if the acceleration region is too small and the grid is too sparse, the ion can arrive at the detector with a significant change in time-of-flight (see Fig. 4) (see Fig. 10 in the Appendix for a zoomed-in view).

SUPPLEMENTARY MATERIAL

See the supplementary material for the complete simulation data tables.

ACKNOWLEDGMENTS

The investigations into the effects of grid morphology was supported by LASP as a part of its efforts into the design of Surface Dust Analyzer (SUDA) instruments under its contract with NASA via its Jet Propulsion Laboratory (JPL), under Contract No. NNN12AAOIC.

AUTHOR DECLARATIONS

Conflict of Interest

The authors have no conflicts to disclose.

Author Contributions

Z. Levin: Conceptualization (lead); Data curation (lead); Formal analysis (lead); Investigation (lead); Methodology (lead); Project administration (supporting); Validation (lead); Visualization (equal); Writing – original draft (lead); Writing – review & editing (lead). **S. Kempf**: Conceptualization (supporting); Formal analysis (supporting); Funding acquisition (lead); Project administration (lead); Resources (lead); Software (lead); Supervision (lead); Visualization (equal); Writing – review & editing (lead).

DATA AVAILABILITY

The data that support the findings of this study are available within the article and its supplementary material.

APPENDIX: ZOOMED-IN VIEWS ON SELECTIVE FIGURES FOR CLARITY

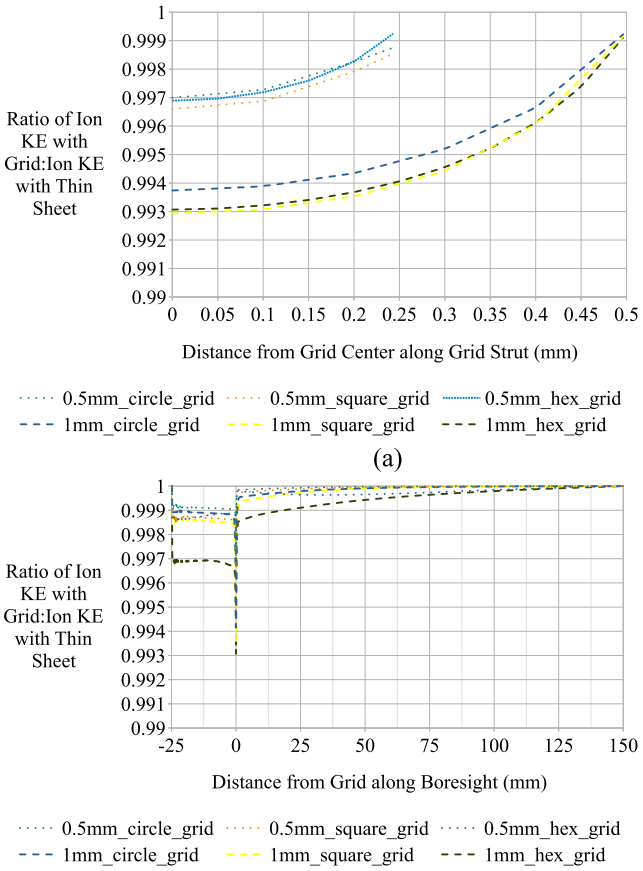

FIG. 8. (a, top) Zoomed-in view of Fig. 3(a). (b, bottom) Zoomed-in view of Fig. 3(b).

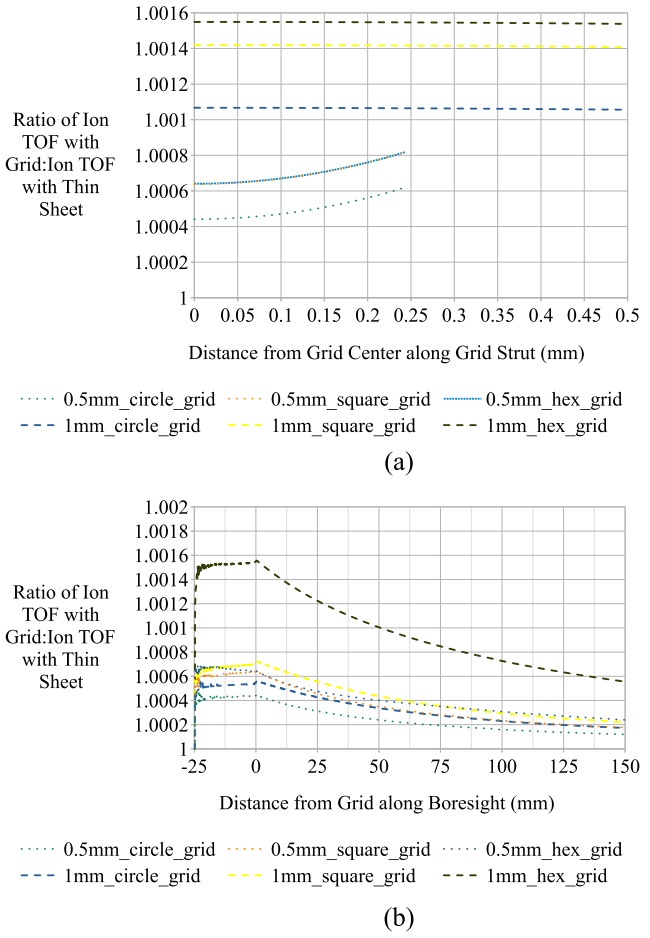

FIG. 10. (a, top) Zoomed-in view of Fig. 4(a). (b, bottom) Zoomed-in view of Fig. 4(b).

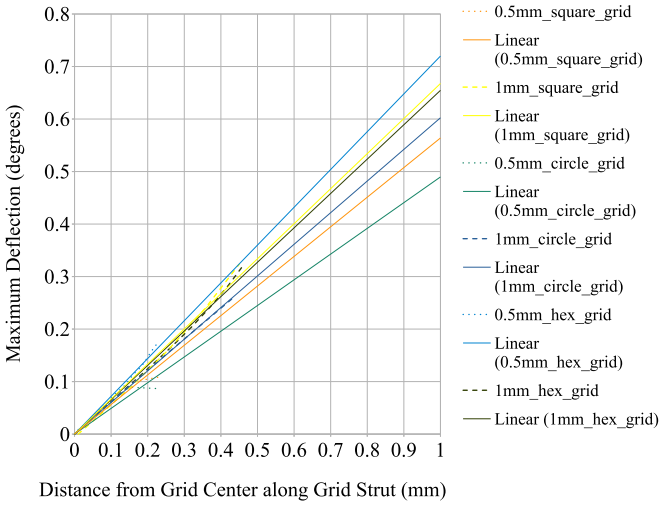

FIG. 9. Zoomed-in view of Fig. 5(a).

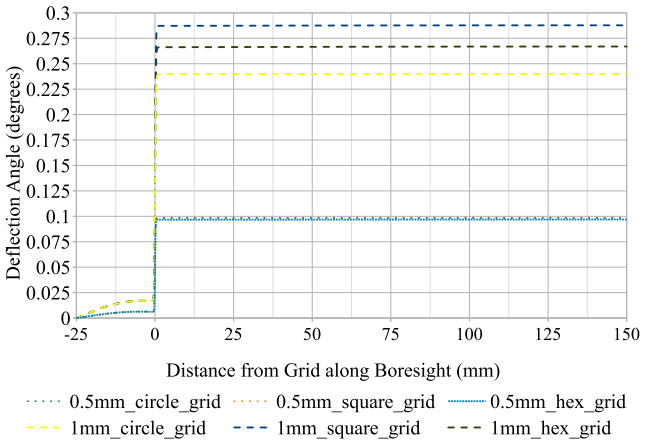

FIG. 11. Zoomed-in view of Fig. 5(b).

REFERENCES

[1]Simion 2019 supplemental documentation, "Grid" Technical Report (Scientific Instrument Services, 2019).
[2]R. King III, "LASER Desorption/LASER Ionization Time-of-Flight Mass Spectrometry Instrument Design and Investigation of the Desorption and Ionization Mechanisms of Matrix-Assisted LASER Desorption/Ionization," Drexel University, 1994.
[3]D. Selby, V. Mlynski, and M. Guilhaus, "Reducing grid dispersion of ions in orthogonal acceleration time-of-flight mass spectrometry: Advantage of grids with rectangular repeat cells," Int. J. Mass Spectrom. **206**(3), 201–210 (2001).
[4]M. Lewin, M. Guilhaus, J. Wildgoose, J. Hoyes, and B. Bateman, "Ion dispersion near parallel wire grids in orthogonal acceleration time-of-flight mass spectrometry: Predicting the effect of the approach angle on resolution," Rapid Commun. Mass Spectrom. **16**, 609–615 (2002).
[5]K. Bamert, R. F. Wimmer-Schweingruber, R. Kallenbach, M. Hilchenbach, B. Klecker, A. Bogdanov, and P. Wurz, "Origin of the May 1998 suprathermal particles: Solar and heliospheric observatory/charge, element, and isotope analysis system/(highly) suprathermal time of flight results," J. Geophys. Res.: Space Phys. **107**, 1130, https://doi.org/10.1029/2001ja900173 (2002).
[6]A. S. Semenov, H. Kessler, A. Liskowsky, and H. Balke, "On a vector potential formulation for 3d electromechanical finite element analysis," Commun. Numer. Methods Eng. **22**, 357–375 (2006).
[7]B. Mamyrin, V. Karatev, D. Shmikk, and V. Zagulin, "The mass-reflectron, a new nonmagnetic time-of-flight mass spectrometer with high resolution," Sov. J. Exp. Theor. Phys. **64**(1), 82–89 (1973).
[8]M. Hilchenbach, "Space-borne mass spectrometer instrumentation," Int. J. Mass Spectrom. **215**, 113 (2002).